In-silico investigation of phytoconstituents from *Plumeria obtusa* and *Sansevieria cylindrica* plants for assessment of anti-venom activity against snake venom

Sunil Shewale[1], Vaishali Undale[1]*, Bhagyashri Warude[2], Vrushali Bhalchim[1], Mohini Kuchekar[3], Jay Gagare[1]

[1] Department of Pharmacology, Dr. D. Y. Patil Institute of Pharmaceutical Sciences and Research, Savitribai Phule University of Pune. Maharashtra (India)

[2] Department of Pharmaceutical Chemistry, Rasiklal M. Dhariwal College of Pharmacy, Savitribai Phule University of Pune. Maharashtra (India)

[3] Department of Pharmacognosy, Modern College of Pharmacy, Nigdi. Savitribai Phule University of Pune. Maharashtra (India).

Author's contribution:

- Sunil Shewale: Conceptualization, study design, experimental work, manuscript preparation, data curation
- Vaishali Undale: Conceptualization, Supervision, critical review for intellectual content, editing
- Bhagyashri Warude: Critical review for intellectual content, editing
- Vrushali Bhalchim- Experimental work and data curation
- Mohini Kuchekar: Critical review for intellectual content, editing
- Jay Gagare: Experimental work and data curation

***Corresponding Author**

Dr. Vaishali Undale,
HOD-Department of Pharmacology,
Dr. D. Y. Patil Institute of Pharmaceutical Sciences and Research Pune,
Maharashtra (India). Pin-411018. Email: vaishali.undale@dypvp.edu.in

Abstract

Background:

Health threat posed by snake bite is one of the most overlooked areas of active research resulting in deaths of thousands of people every year in many impoverished nations. Therefore, improvement of available therapeutic options along with development of other treatment choices is important for snakebite management which could help in reducing the mortality, and morbidity. Taking this in view, the *in-silico* study was conducted.

Aim: To investigate the interaction of phytoconstituents from *Plumeria obtusa* and *Sansevieria cylindrica* plants with various proteins for assessment of anti-venom activity against snake venom.

Methods: A protein data bank was searched for various important enzymes found in different snake venoms, and were saved in the PDB file. The plant phytoconstituents were selected from published literatures. Structure of phytoconstituents were drawn using Chem Draw software and

converted to SDF files. The selected proteins, and phytoconstituents were subjected to docking using the iGEMDOCK software. The docking results were then validated through AutodockVina and the interactions were visualised through Biovia Discovery Studio Visualizer. Docking results were also compared with selected standard inhibitor of docked proteins.

Results: Many plant phytoconstituents showed good binding affinity and were able to form H-bonds, alkyl, π-alkyl, Van der Waals, and π-sigma bonds with the active-site residues of 1B41, 1CJY, 2JGA, 4TKX, 4UFQ, and 5NJB proteins.

Conclusion: Docking result interpreted the possible pharmacological activity of plant phytoconstituents against the snake-venom through inhibition of respective macromolecules.

Keywords: *Molecular docking, Plumeria obtusa, Sansevieria cylindrica, Snake venom, Enzymes.*

Introduction

Snakebite is a major life-threatening disease of many tropical, and subtropical provinces particularly; Sub-Saharan Africa, Southeast Asia, and Latin America.[1] An estimated 5.4 million cases, 2.7 million poisonous cases, and 0.08 to 1.37 million death occurs annually because of snake bites.[2] Indian cobra (*Naja naja*), Russell's viper (*Daboia russelii*), common krait (*Bungarus caeruleus*), and the saw-scaled viper (*Echis carinatus*) snakes are among the several poisonous snakes found in India and many other countries. They produce the most severe local tissue damage at the bite site.[3]

Snake venoms are complex mixture; made up mostly of proteins, and peptides with a wide range of biological actions.[4] The venom components with haemorrhagic activity are snake venom metalloproteinases (SVMPs), which are both direct and indirect mediators of local tissue damage such as bleeding, edema, myonecrosis, dermonecrosis, and inflammation after envenoming.[5] The majority of venom metalloproteinases are fibrinogenolytic enzymes that preferentially cleave the A-chain of fibrinogen while slowly cleaving the B-chain. Casein, insulin B peptides, and intermolecularly quenched fluorogenic peptide substrates have all been used to test metalloproteinase substrate specificities.[4] Hemorrhage produced by any enzymatic toxins can subsequently lead to edema, shock, tissue necrosis, and reduced ability to regenerate muscle tissue.[6] Additionally, leakage of blood from affected vessels also helps spread other venom toxins to their target tissues. Phospholipase A2 (PLA2), Snake Venom Serine Proteases (SVSP), 5'-nucleotidase, Hyaluronidase, Acetylcholinesterase, and Three Finger Toxins (3FTx) are also considered dominant protein families responsible for toxic effect in human being. Therefore, it can be hypothesized that the inhibition of these enzymes may result in a significant overall reduction in damage following envenomation.[7]

ASV therapy is best available cure against snake envenomation, but it is expensive, not readily available and has risk of immunological reactions.[8] These factors necessitate complementary therapies to treat snakebites. The treatment of snake envenomation using plants and folk medicine is old and ancient practice in many poor communities from rural areas.[9] Moreover, many evidences support the pharmacological use of plants, its extracts and isolated compounds against snakebites as medicine.[1,10]

Computational biology and bioinformatics have the potential to accelerate drug discovery and repurposing process. This involves prediction and scoring of binding free energy in between target and desired molecule by molecular docking. *In-silico* approaches have paved the way for the solution of many biological problems, leading to the discovery of novel inhibitors against a variety of diseases. The present study investigates the molecular interaction between selected phytoconstituents from published literature of *Plumeria obtusa* (PC) and *Sansevieria cylindrica* (SC) plants with amino acids residues of target proteins for potential snake venom enzymes inhibition.

Material and Methods

Protein preparation

A Protein Data Bank (PDB) was search for human acetylcholinesterase, glycosylated protein, human cytosolic phospholipase, human cytosolic 5'-nucleotidase III, Protease, and E. coli using Research Collaboratory for Structural Bioinformatics (RCSB) (https://www.rcsb.org/). The criteria for choosing PDBs were based on highest possible resolution. The resolution ensures that the 3D structures used for docking are of high quality, and that the structure is free of mutations, as mutations can have a significant impact on the final confirmation of a protein complex with ligand. Preparation of the proteins was carried out with the Biovia Discovery Studio Visualizer (DSV) 2017 (Prepare protein protocol). Protein preparation entailed adding hydrogen atoms, defining bond orders, deleting unwanted water molecules and salts, and optimising the hydrogen bond network. As protein functions as monomer, protein chains other than standard drug interacting chains were removed. Polar hydrogens were added to optimize the hydrogen-bonding network. The proteins were minimised in terms of energy and active sites were predicted with the selection of maximized GRID parameters using DSV. Finally, the prepared structure of protein was saved in the PDB file format for docking. Details of the selected PDB are mentioned in Table 1.[11-16] Also, the cartoon ribbon model of each protein is displayed in figure 1.

Table 1: List of selected PDB with PDB code, ligands and resolution

S.N.	PDB Code	Target	Ligand	Resolution
1.	1B41	Human acetylcholinesterase	Physostigmine	2.76 Å
2.	1CJY	Human cytosolic phospholipase a2	Indomethacin	2.50 Å
3.	2JGA	Crystal structure of human cytosolic 5'-nucleotidase III	Vanillic acid	3.01 Å
4.	4TKX	Protease	Remdesivir	1.60 Å
5.	4UFQ	Hyaluronidase	Tannic acid	1.65 Å
6.	5NJB	E. Coli Microcin-processing metalloprotease	Batimastat	1.50 Å

Figure 1: Cartoon ribbon model of selected proteins

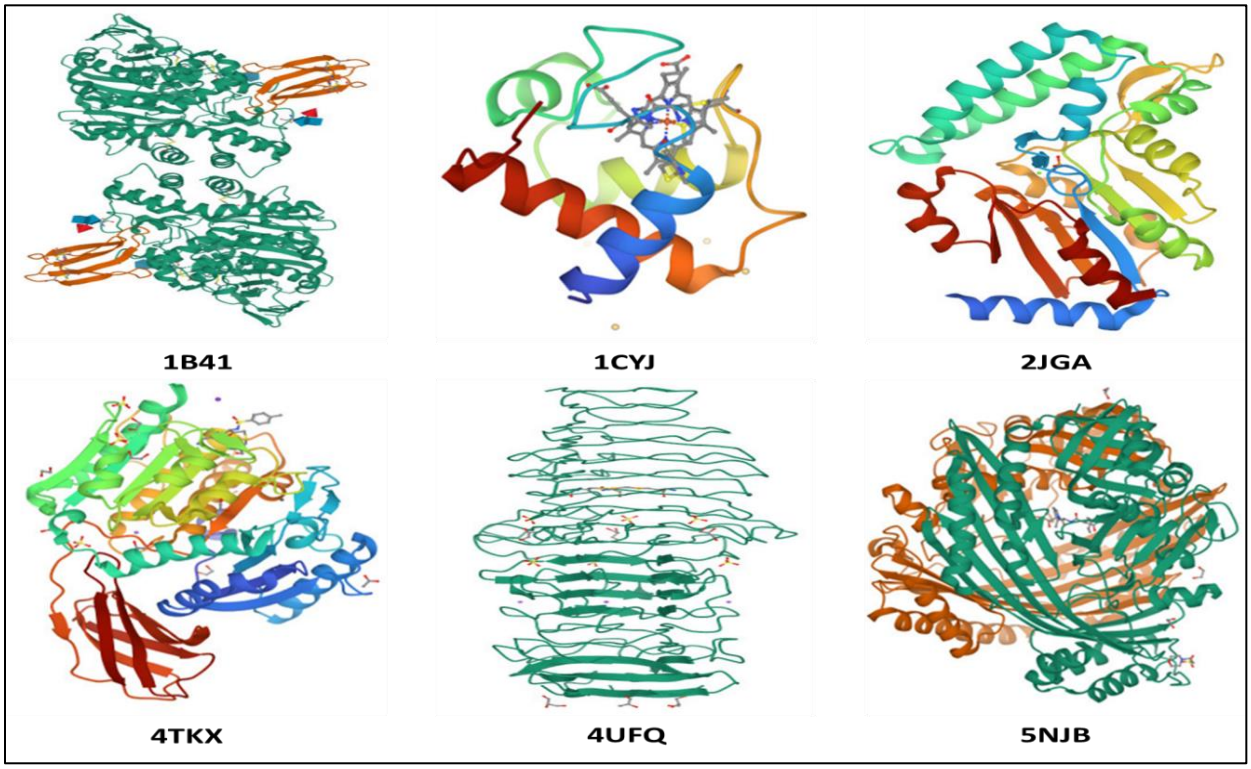

Phytoconstituents and ligands structure preparation

In this study, eight compounds from *Plumeria obtusa* plant and ten compounds from *Sansevieria cylindrica* plant available from published literature were used for docking studies.[17-18] All standard drugs were retrieved from PubChem database (https://pubchem.ncbi.nlm.nih.gov/). Structure of phytochemical constituents were drawn using Chem Draw Ultra 12.0 software and converted to SDF file. Open Babel tool was used for optimizing designed phytochemical constituents with force fields MMFF94, and GHEMICAL. Energy minimisation of all the phytochemical constituents was done by Conjugate Gradient and Steepest Descent optimization algorithms. The cycle had 50000 steps and a convergence criterion of 0.001 kcal/mol/Angstrom. Finally, all ligand option was used to convert the minimised files to PDBQT format in order to generate their atomic coordinates, which were used as input in PyRx software (http://PyRx.sourceforge.net). The list of phytoconstituents, their codes and PubChem ID is given in Table 2.

Table 2: List of Phytoconstituents/ ligands with PubChem ID and manual code

Phytoconstituents							
Plumeria obtusa				***Sansevieria cylindrica***			
S. N.	**Code**	**Ligand**	**Pub Chem ID**	**S. N.**	**Code**	**Ligand**	**Pub Chem ID**
1.	PC1	Steroid U	133659	1.	SC1	Dihydrochalcone	64802

2.	PC1a	beta-Amyrin	73145	2.	SC2	Pongol methyl ether	636768
3.	PC1b	Triterpenoid	451674	3.	SC3	Homopterocarpin	101795
4.	PC2	Lupeol	259846	4.	SC4	1-Phenylpropane-1,3-diol	572059
5.	PC2a	Plumieride	72319	5.	SC5	p-Coumaroyl tyramine	5372945
6.	PC2b	alpha-Amyrin	73170	6.	SC6	7,4'-dihydroxy-homoisoflavanone	3759709
7.	PC3	Ursolic acid	64945	7.	SC7	N-trans-Feruloyloctopamine	24096391
8.	PC3a	Triacetin	5541	8.	SC8	3,4-Dihydroxyallylbenzene	53446942
				9.	SC9	3-Hydroxychavicol 1-glucoside	78384828
				10.	SC10	27-p-Coumaroyloxy ursolic acid	5459189

Identification of Cavity and Active Amino Acid Residues

Phytochemical constituents from *Plumeria obtusa* and *Sansevieria cylindrica* plants and proteins were imported in AutoDock Vina Wizard and macro molecules converted into PDBQT format. The three dimensional grid box for complex with standard ligand and protein (size_x = 102.708; size_y= 110.001; size_z =135.04),(size: x = 49.920; y = 14.42; z =56.75), (size: x = 32.392; y = 21.009; z =12.77), (size: x = 28.89; y = 19.48; z =5.715) (size: x = 141.220; y = 8.78; z =91.38) (size: x = 37.68; y = 71.109; z =56.63) were generated automatically for 1B41, 1CJY, 2JGA, 4TKX, 4UFQ, and 5NJB, respectively. Using the Toggle Selection Sphere option, the active amino acid residues were chosen to define the cavity. The grid box was aligned in a way that it occupied all of the active binding sites and essential residues. The three-dimensional grid boxes were generated.[19-20]

Docking procedure

Rapid Protein-Ligand docking was performed using the software iGEMDOCK version 2.1. iGEMDOCK is a Drug Design System for molecular docking and screening by BioXGEM labs. iGEMDOCK outputs hydrogen bond, electrostatic, and Van Der Waals [VdW] forces. These trials were each docked with 70 generations and 1 solution. The post-docking tool was then used to find the docking poses and energy values. iGEMDOCK uses scoring function and Generic Evolutionary Method for molecular docking. It has a graphical user interface that recognizes the pharmacological interactions and performs virtual screening. The docking results were then validated through AutodockVina and the interaction was visualised through Biovia Discovery Studio Visualizer.

Molecular docking of 1B41, 1CJY, 2JGA, 4TKX, 4UFQ, and 5NJB with phytochemical constituents from *Plumeria obtusa* and *Sansevieria cylindrica* were subjected to docking using AutodockVina Wizard of PyRx virtual screening 0.8 version software to find the reasonable

binding geometry and discover the protein-ligand connections. Docking predicted non-bonded, non-covalent interactions between a receptor or active site region of a protein and a drug or chemical molecule forming an intermolecular complex. The final docking result includes affinity prediction (scoring) for the molecules investigated, resulting in a relative rank ordering of the docked compounds in terms of affinity, reported as kcal/mol.[21] A greater negative binding energy indicates a greater binding affinity. DSV was used to analyse binding interactions on complexes with higher docked scores.

Results and Discussion

Molecular docking using iGEMDOCK software

The docked poses of the molecules were represented in Figure 2 and 3 (a,b,c,d,e,f). All the molecules have shown inhibition against the respective macromolecules. The binding energy represents that lower the binding energy better is the interaction (Table 3 and 4).

The results of molecular modelling using a molecular docking method revealed the possible molecular orientation of the *Plumeria obtusa*, and *Sansevieria cylindrica*. All docked conformations revealed the strong H-bond with an oxygen atom of Glu143 side chain and another interaction with some residues in the active site. From the docked conformation of PC, H-bond interactions were also found with Lys110, Ala111, Tyr112, His146, and Arg151. The closest distance between Zn2+ atom and SC's atom were 3.89 Å, which was the distance between Zn2+ atom and O9 atom of PC. In case of SC, the O9 atom of docked conformation showed an interaction with the Zn2+ atom with a distance of 2.41 Å.[3]. The H-bond interactions generated with Asn106, Ile108, Gly109, His152, and Ser169 were the other interactions.[22] The docked PGG conformation exhibited a comparable interaction between the docked PC and SC conformations, as shown in Asn106, Ile108, Gly109, Lys110, Ala111, Tyr112, Arg151, His152, and Ser169 all had H-bond interactions. H-bond interactions with Lys105, Ile107, Leu113, Asp114, His142, Val150, His170, and Ile171 were also discovered.[23]

Table 3: Binding energy and other parameters for ligands from *Plumeria obtusa* against various proteins

Compound	Total Energy	VDW	H-Bond	Aver. Con. Pair
1B41 (Acetylcholinesterase)				
PC1	-118.354	-106.979	-11.3751	20
PC1a	-105.903	-88.2089	-17.6943	14.6458
PC1b	-113.798	-106.798	-7	17.0612
PC2	-108.367	-94.089	-14.2781	16.0233
PC2a	-113.78	-107.049	-6.73069	14.5283
PC2b	-133.939	-117.036	-16.9035	17.7115
PC3	-111.053	-102.344	-8.70872	17.561
PC3a	-109.464	-90.4014	-19.0628	14.76

ICJY (Phospholipase A2)				
PC1	-103.402	-95.3439	-8.05776	16
PC1a	-94.0357	-94.0357	0	15.3333
PC1b	-108.204	-98.9976	-9.20603	15.449
PC2	-127.084	-127.084	0	20
PC2a	-127.745	-111.501	-16.2441	16.4528
PC2b	-111.013	-107.377	-3.63662	14.4231
PC3	-104.534	-98.7358	-5.79785	17.6829
PC3a	-117.961	-115.705	-2.25558	18.06
2JGA (5'-nucleotidase)				
PC1	-123.638	-114.138	-9.5	19.7143
PC1a	-96.2033	-88.0689	-8.13439	14.6458
PC1b	-106.93	-97.5839	-9.3459	13.7143
PC2	-105.441	-90.4165	-15.0247	14.8372
PC2a	-127.822	-104.237	-23.5851	16.0377
PC2b	-116.13	-101.016	-15.1143	14.4808
PC3	-109.276	-95.8865	-13.3892	19.3659
PC3a	-114.345	-107.437	-6.90803	15.4
4TKX (Protease)				
PC1	-113.741	-104.461	-9.27914	17.881
PC1a	-124.176	-113.87	-10.3062	17.5833
PC1b	-112.587	-104.072	-8.51455	15.7347
PC2	-116.968	-110.873	-6.09463	19.0698
PC2a	-121.519	-108.444	-13.0746	15.2642
PC2b	-129.337	-116.588	-12.7485	18.5192
PC3	-132.82	-120.458	-12.3617	21.6341
PC3a	-126.542	-120.06	-6.48217	20.1
4UFQ (Hyaluronidase)				
PC1	-104.957	-91.6141	-13.3433	17.5952
PC1a	-108.264	-105.112	-3.15213	14.3958
PC1b	-105.869	-102.369	-3.5	13.6327
PC2	-96.844	-88.3359	-8.50801	14.093
PC2a	-115.4	-106.139	-9.26071	15.0755
PC2b	-114.354	-109.64	-4.7139	15.4038
PC3	-110.176	-109.369	-0.80716	18.7073
PC3a	-115.412	-113.011	-2.40067	18.06
5NJB (Metalloprotease)				
PC1	-103.815	-100.742	-3.07251	18.4524

PC1a	-116.05	-112.55	-3.5	15.9583
PC1b	-114.871	-106.687	-8.18344	17.0408
PC2	-111.972	-107.53	-4.4417	17.9535
PC2a	-120.017	-104.949	-15.0676	15.3962
PC2b	-116.32	-104.707	-11.6133	15.7308
PC3	-99.6962	-99.6962	0	17.6829
PC3a	-105.192	-95.6923	-9.5	13.96

Table 4: Binding energy and other parameters for ligands from *Sansevieria cylindrica* against various proteins

Compound	Total Energy	VDW	H-Bond	Aver. Con. Pair
1B41 (Acetylcholinesterase)				
SC1	-94.4975	-84.3808	-10.1167	26.9565
SC2	-94.0649	-85.6193	-8.44559	25.7826
SC3	-64.8995	-52.4708	-12.4287	33.9091
SC4	-82.2577	-76.0962	-6.16149	35.5714
SC5	-91.4364	-88.6946	-2.74183	26.5
SC6	-98.2441	-90.7378	-7.50636	25.4167
SC7	-91.2533	-87.2842	-3.96914	28.15
SC8	-89.0004	-85.0445	-3.95589	33.9048
SC9	-96.9088	-90.3682	-6.54063	25.9167
SC10	-76.784	-74.5632	-2.22083	24.2381
ICJY (Phospholipase A2)				
SC1	-72.4943	-63.6154	-8.87882	18.2609
SC2	-89.4013	-85.9013	-3.5	24.8696
SC3	-62.6409	-54.2461	-8.39472	29.7273
SC4	-84.2376	-79.7753	-4.46232	25.2381
SC5	-87.9742	-79.3965	-8.57763	23.5
SC6	-78.3483	-72.7678	-5.58053	24.4583
SC7	-80.6576	-77.1576	-3.5	27.75
SC8	-89.1459	-87.159	-1.98684	30.1429
SC9	-99.3415	-99.3415	0	25.5833
SC10	-83.5476	-81.0476	-2.5	25.5714
2JGA (5'-nucleotidase)				
SC1	-89.9708	-83.9755	-5.99538	25.2174
SC2	-92.8537	-84.8194	-8.03432	25.1304
SC3	-70.7328	-50.603	-20.1297	31.2727

SC4	-86.4912	-75.3766	-11.1146	21.9048
SC5	-89.9648	-74.6129	-15.352	22.8636
SC6	-79.0159	-69.0751	-9.94082	19.3333
SC7	-84.8637	-80.591	-4.27266	24.8
SC8	-79.7072	-76.2185	-3.48869	22.7619
SC9	-91.5195	-73.6533	-17.8662	26.2083
SC10	-84.9458	-82.4458	-2.5	28.0476
4TKX (Protease)				
SC1	-84.7972	-76.0937	-8.7035	21.7391
SC2	-94.0868	-87.0868	-7	23.6957
SC3	-75.9394	-63.9878	-11.9515	33.9091
SC4	-88.0358	-81.3944	-6.64136	25.9048
SC5	-95.8535	-82.8535	-13	27.4091
SC6	-86.5771	-76.4183	-10.1589	23.75
SC7	-103.094	-91.9196	-11.1748	30.55
SC8	-98.1418	-90.2179	-7.92387	26.4762
SC9	-107.67	-93.5163	-14.1538	33.9583
SC10	-108.8235	-96.384	-11.43952	23.8571
4UFQ (Hyaluronidase)				
SC1	-84.9835	-79.8251	-5.15843	20.9565
SC2	-87.1644	-71.1971	-15.9673	21.5217
SC3	-87.5127	-71.2034	-22.3093	25.2727
SC4	-77.5721	-66.4567	-11.1154	20.2857
SC5	-74.1975	-71.1766	-3.02093	23
SC6	-78.5002	-71.5002	-7	19.5833
SC7	-82.3192	-82.1316	-0.18759	24.5
SC8	-80.116	-63.8553	-16.2608	25.7619
SC9	-82.2815	-78.7815	-3.5	20.75
SC10	-72.6923	-68.9364	-3.7559	22.9524
5NJB (Metalloprotease)				
SC1	-87.2851	-79.7515	-7.53357	24.0435
SC2	-81.5079	-72.6505	-8.85744	23.3913
SC3	-66.9675	-55.7069	-11.2606	34.2727
SC4	-92.6081	-82.1172	-10.4909	25.8571
SC5	-85.9025	-73.9947	-11.9078	21.7273
SC6	-87.8721	-65.167	-22.705	22.8333
SC7	-83.3489	-75.5674	-7.78148	28.45
SC8	-78.9493	-75.5366	-3.4127	23.8095

SC9	-86.1886	-76.9388	-9.2498	23.0833
SC10	-93.9254	-82.4875	-6.43795	24.9524

Figure 2: Binding interaction of ligands from *Plumeria obtusa* with various proteins

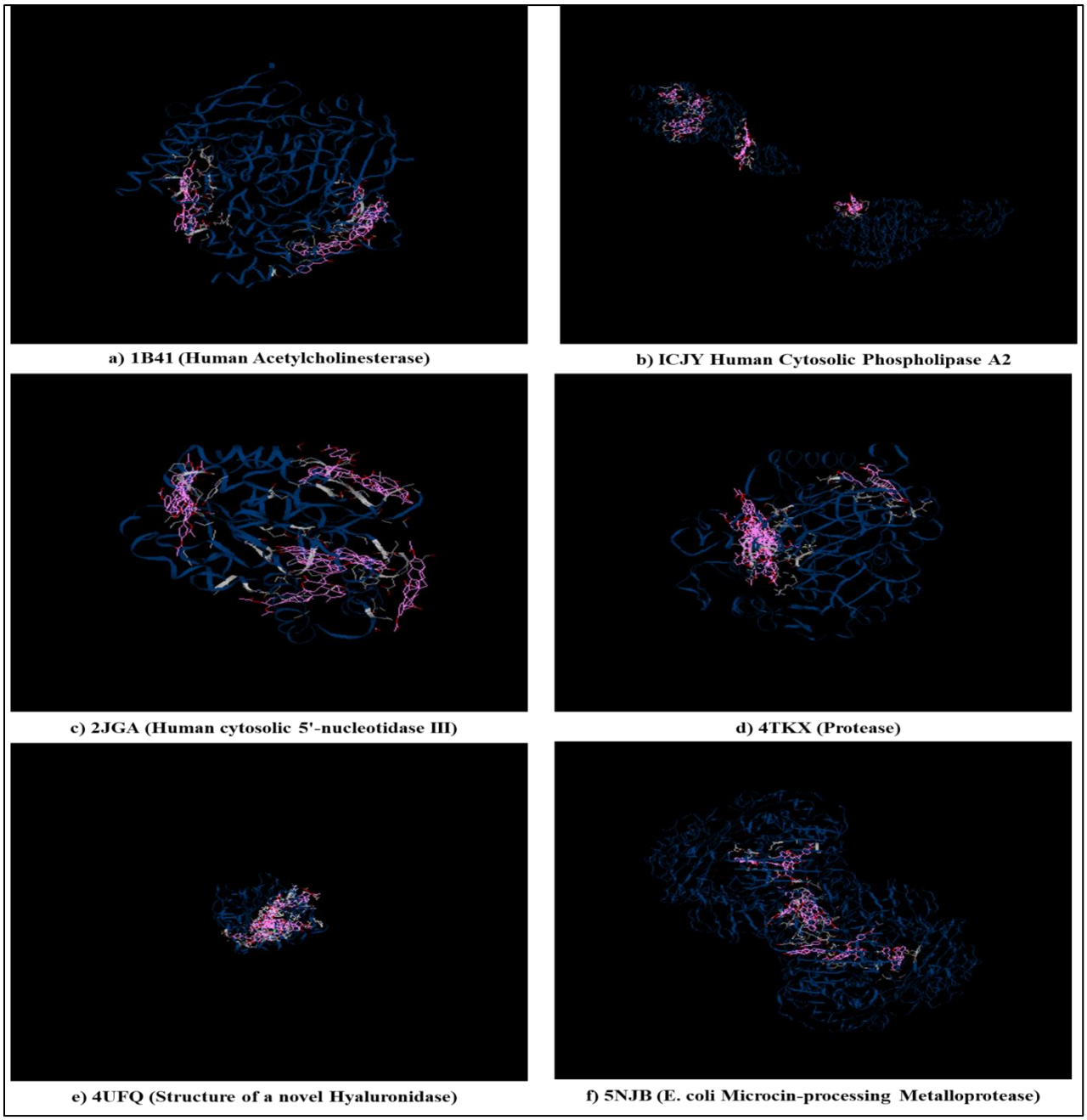

Figure 3: Binding interaction of ligands from *Sansevieria cylindrica* with various proteins

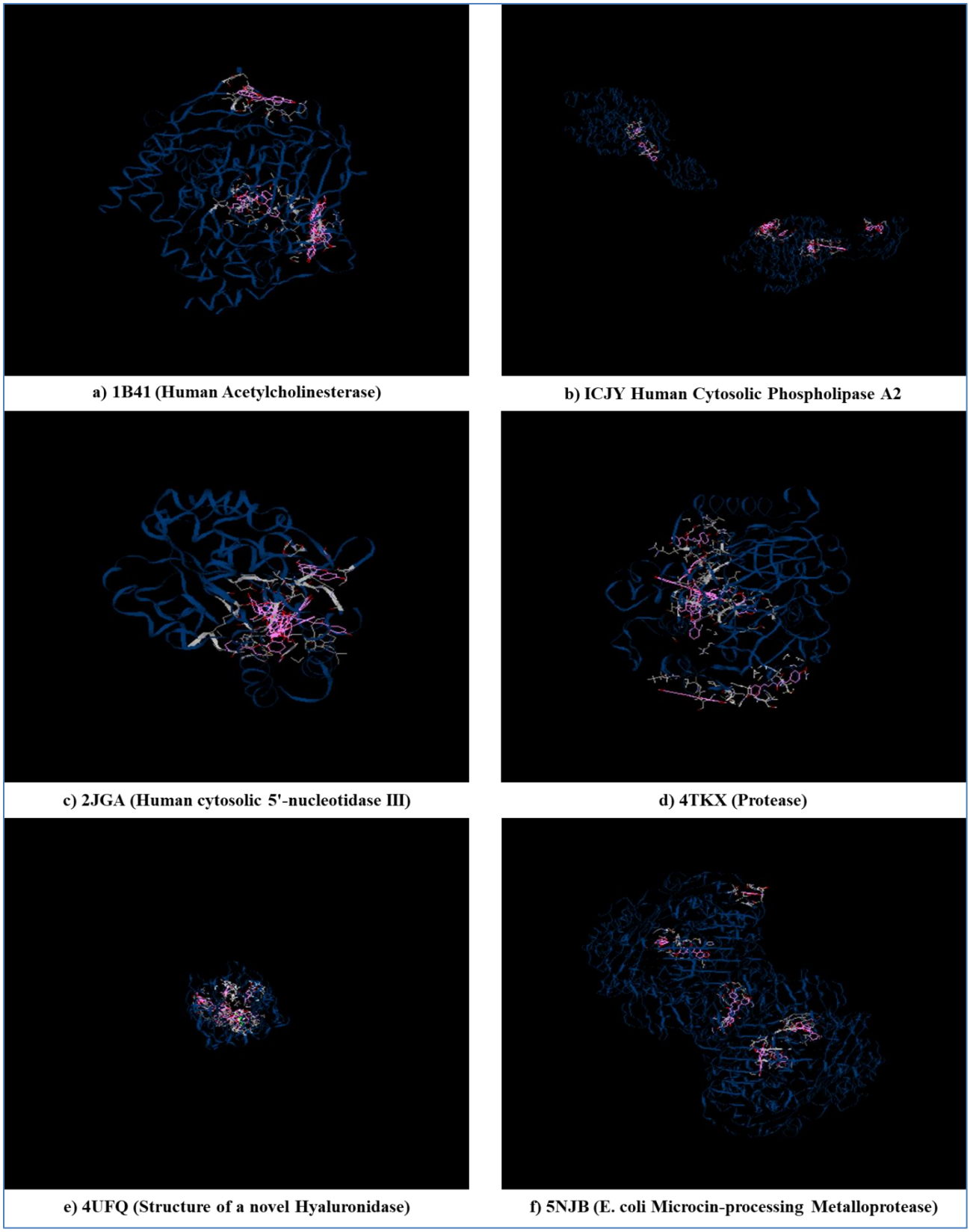

a) 1B41 (Human Acetylcholinesterase)

b) ICJY Human Cytosolic Phospholipase A2

c) 2JGA (Human cytosolic 5'-nucleotidase III)

d) 4TKX (Protease)

e) 4UFQ (Structure of a novel Hyaluronidase)

f) 5NJB (E. coli Microcin-processing Metalloprotease)

Molecular docking using AutodockVina software

Phytochemical constituents from *Plumeria obtusa* and *Sansevieria cylindrica*, were docked with PDB 1B41, 1CJY, 2JGA, 4TKX, 4UFQ, and 5NJB in the targeted cavity. Out of the 18 molecules some molecules shown very good binding affinity like SC10 with 1B41 – 8.9 kcal/mol, 4TKX -8.3 kcal/mol, 5NJB -11.2 kcal/mol, ligand SC2 with 2JGA -9.8 kcal/mol and ligand SC3 with 4UFQ -8.4 kcal/mol. Ligands of PC and SC interactions with active amino acid residues are shown in Table 5. Docking poses of phytochemical constituents of PC and SC with 1B41, 1CJY, 2JGA, 4TKX, 4UFQ, and 5NJB PDB in 2D-poses along with the number of hydrogen bonds involved in the interaction are shown in figure 4 (a,b,c,d,e,f,g,h,i,j,k,l). The shown images focus on the interactions of functional groups on ligands with active amino acid residues in the targeted cavity. Some of the better docking poses with ligands of PC and SC established a network of molecular interactions (H-bonds, Van der Waals, alkyl, π-alkyl, and π-sigma bonds) with the active-site residues of 1B41, 1CJY, 2JGA, 4TKX, 4UFQ, and 5NJB. It established various binding interactions including conventional H-bonds TYR 124 (2.36), TRP 102 (6.40) GLY 155 (3.81), THR 240 (4.13) ASN 551 (4.84), THR 240 (4.13), ASN 551 (4.84), SER 669 (3.53), SER 195 (4.54) HIS 57 (5.95), ARG 184 (4.40), ARG 306 (6.84), π-alkyl (Leu354, Trp 383, Leu 536, Leu 391), pi-pi stack TRP 215 (7.14), CYS 191 (5.47), TYR 341 (6.2 A), TRP 286 (5.45), HIS 57 (4.85 and 4.65 A), Van der Waals interaction ASP 189 (5.28) etc.

Comparison with the standard Vanillic acid and phytochemical constituent SC2 with 2JGA shows promising interaction with TRP 102, HIS 57, SER 106, TYR 103 at the active domain as human cytosolic 5'-nucleotidase III inhibition. 2D pose of 4TKX with Remdesivir and SC10 observed similar interaction on amino acid TYR 238, ASP 548, SER 669, ASN 551, and ARG 668 at active domain for inhibition of protease. As compared to Tannic acid docking interaction on 4UFQ, phytoconstituent SC3 shows promising hydrogen bonding with SER 195, HIS 57, pi-pi stack TRP 215 and CYS 191, alkyl pi interaction with TRP 60 and vander walls interaction with Val 213, SER 214, and GLY 226 indicating hyaluronidase inhibition activity. Docking interaction of SC10 compared with Batimastat with 5NJB have more promising hydrogen bonding interaction on amino acid ARG 351, 184, 306, 207, SER 160, GLN 41, and SER 43 etc for metalloprotease inhibition activity. Vander walls interactions are observed with the complex of Piperine and 1CJY protein at amino acid SER (48), GLU (47), GLU (54), LYS (45), GLY (42) at the active site domain. As compared with Piperine interaction phytochemical constituent SC6 shows promising interaction like hydrogen bonding interaction with GLY (551) and Vander walls interaction with GLU, GLY, LYS, ALA, and SER etc.

Figure 4: 2D diagrams of ligand & protein complexes

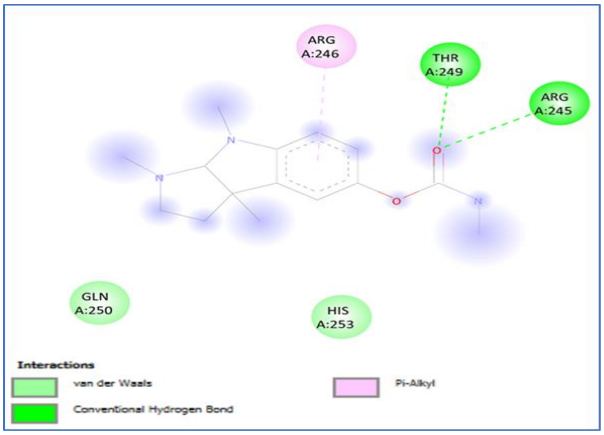

(a) 2D pose of 1B41 with Physostigmine

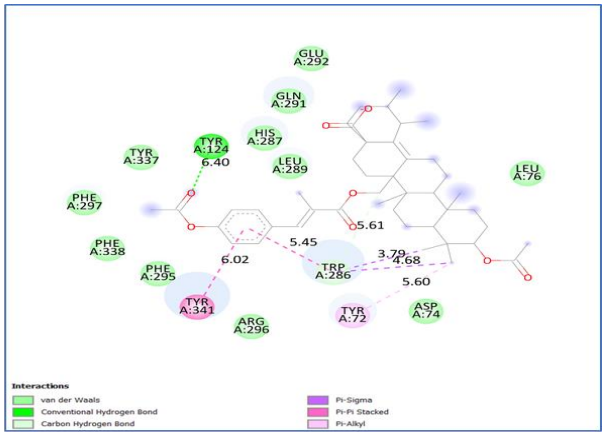

(b) 2D pose of 1B41 with SC10

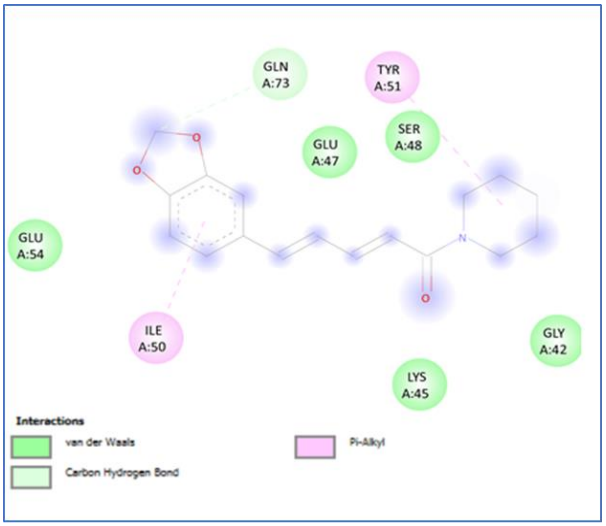

(c) 2D pose of 1CJY with Piperine

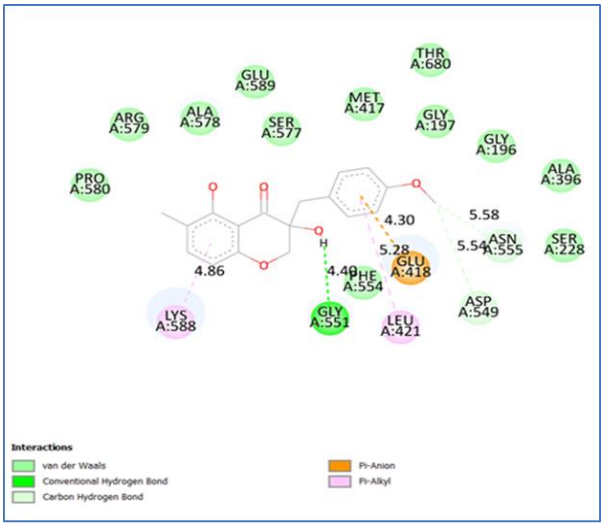

(d) 2D pose of 1CJY with SC6

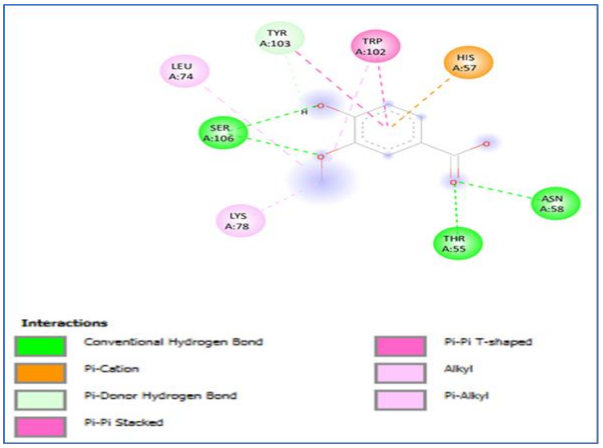

(e) 2D pose of 2JGA with Vanillic acid

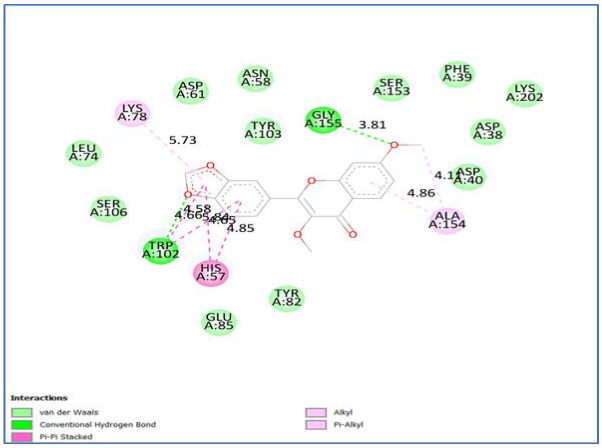

(f) 2D pose of 2JGA with SC2

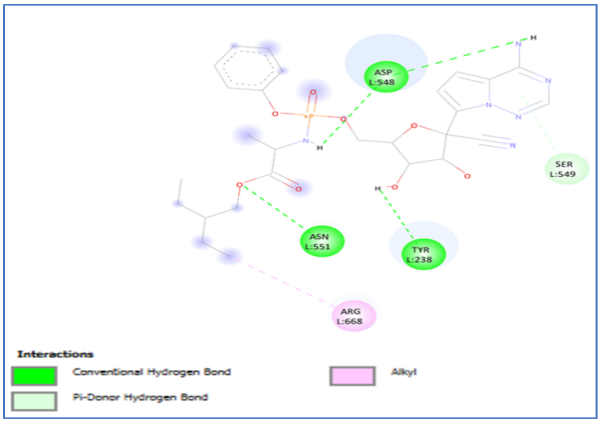

(g) 2D pose of 4TKX with Remdesivir

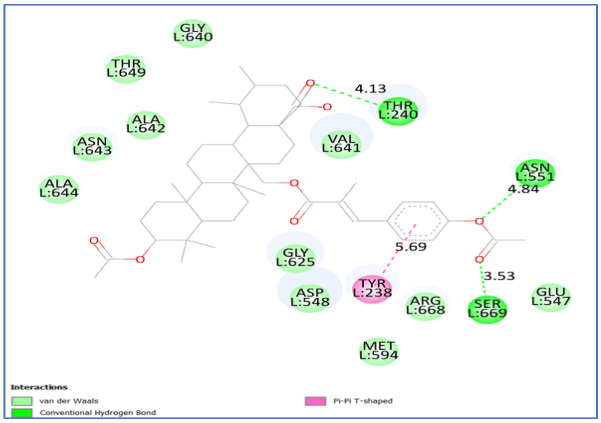

(h) 2D pose of 4TKX with SC10

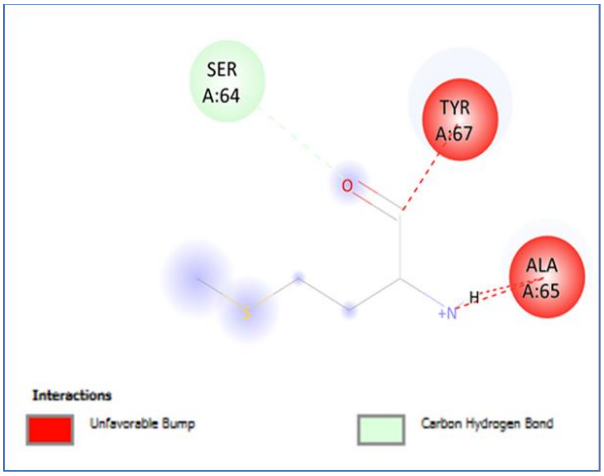

(i) 2D pose of 4UFQ with Tannic acid

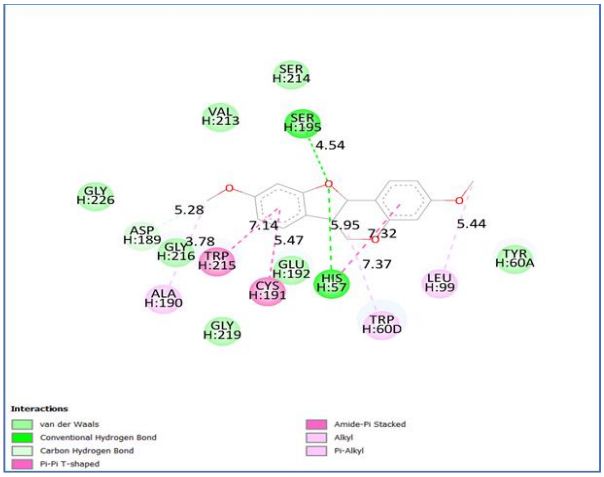

(j) 2D pose of 4UFQ with SC3

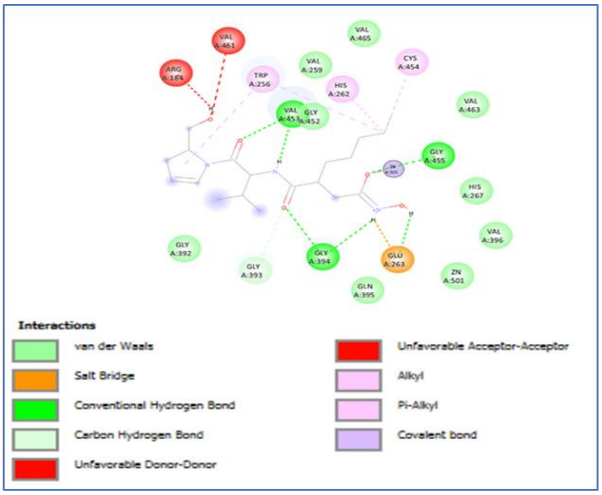

(k) 2D pose of 5NJB with Batimastat

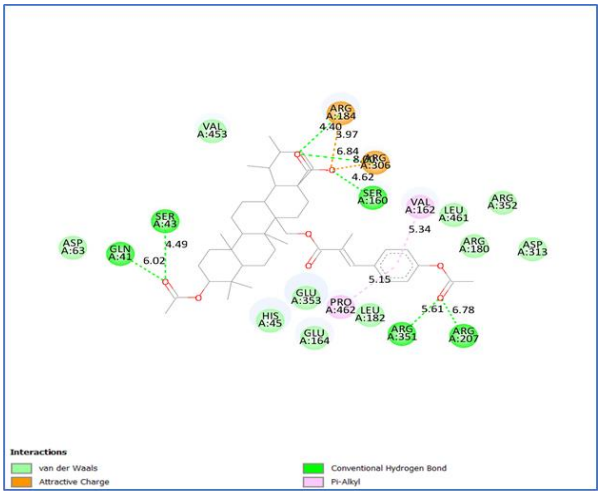

(l) 2D pose of 5NJB with SC10

Table 5: Standard and Plant phytoconstituents interactions with amino acid residues of protein

Ligand	Protein id	Binding Energy	Interaction
Physostigmine	1B41	-6.5	H bonding -ARG 245(2.32), THR 249(1.98) pi-alkyl – ARG 246(3.77)
SC10	1B41	-8.9	H bonding -TYR 124(2.36) pi-pi stack HIS 57(4.85 and 4.65 A) pi-sigma interaction TRP 286 (3.79) (4.68)
Piperine	1CJY	-5.4	Pi-alkyl – TYR 51(3.61) Van der waals – GLN 73(5.15)
SC6	1CJY	-5.1	H-bonding – GLY 551(4.40) Pi-anion – GLU 418(4.30) Pi-alkyl – LEU 421(5.28), LYS 588(4.86) Van der waals – ASN 555(5.58), ASP 549(5.54)
Vanillic acid	2JGA	-6.3	H-bonding -THR 55(2.11), ASN 58(2.53), SER 106(2.47), TYR 103(2.9) pi-pi stack HIS 57(4), TRP 102(4.52): TYR 103(5.2), TRP 102(4.52) Pi alkyl – TRP 102(4.69) Alkyl – LYS 78(4.06), LEU 74(4.7)
SC2	2JGA	-9.8	H bonding -TRP 102 (6.40) GLY 155 (3.81) pi-pi stack TYR 341(6.2 A) TRP 286 (5.45) pi-sigma interaction LYS 78 (5.73) ALA 154(4.86 and 4.11 A^0)
Remdesivir	4TKX	-7.1	H bonding ASN 551(2.26), ASP 548(2.22), ASP548(1.82), TYR238(2.51) Pi-donor – SER549(3.44) Alkyl - ARG668(4.23)
SC10	4TKX	-8.3	H bonding -THR 240(4.13) ASN 551 (4.84) SER669 (3.53) pi-pi stack TYR 338(5.69A)
Tannic acid	4UFQ	-5.6	H bonding –SER64(3.17)
SC3	4UFQ	-8.4	H bonding -SER 195(4.54) HIS 57 (5.95) Van der waals-ASP189(5.28) Amide Pi stack-CYS189(5.47) TRP215(7.14) pi-pi stack TRP 215(7.14) CYS 191(5.47)
Batimastat	5NJB	-8.5	H bonding - GLY394(2.33), VAL453(1.9), GLY455(2.05), GLY394(2.18), GLU263(1.82), VAL453(1.88), GLY393(3.03)

			Pi alkyl- TRP256(5.03), TRP256(5.12), TRP256(4.65), HIS262(4.09); Salt bridge - GLU263(2.48); Alkyl - CYS454(4.75)
SC10	5NJB	-11.2	H bonding –ARG184 (4.40) ARG306 (6.84) SER47(4.49) SER160(4.62) ARG351 (5.61) ARG207(6.78) GLN41(4.49) SER 43(6.02) Pi alkyl- PRO462(5.15) VAL 162(5.34)

Conclusion

Docking result interpreted the promising pharmacological activities against various snake venoms toxins. Prominent discovery tools in science and engineering, widely adopted in applications ranging from drug discovery to materials design. The fidelity of the predictions of molecular simulations hinges on the reliability and accuracy of the chosen force fields. The current study is an effort to identify anti-venom activity by PC and SC phytochemical constituents that may be considered for drug development to treat snakebite. The binding energy of the ligand and its receptor quantifies the efficiency of the ligand-protein complex. The similar results are obtained by iGEDOCK and Autodock software which support the outcome of the docking study. Taken together, we therefore suggest that the SC2, SC3, SC6 and SC10 ligands could act as potential inhibitors against the snake venom activity. In future, the molecular dynamic study by molecular simulation will be useful for understanding the prominent mechanism of action of phytoconstituents.

Conflict of Interest

The authors declared no potential conflicts of interest with respect to the research, authorship, and/or publication of this article.

Funding

The authors received no financial support for the research, authorship, and/or publication of this article.

References

1. Shewale S, Undale V, Chitlange S, et al. Ophidian Bite: The Balance Between Perception, Idealism and Realism. *Trop. J. Nat. Prod. Res*. 2021; 5(7):1166-1178. doi: https://doi.org/10.26538/tjnpr/v5i7.1
2. World Health Organization. Snakebite envenoming. Key facts. [Online]. 2021. [cited 2021 May 17]. Available from: https://www.who.int/news-room/fact-sheets/detail/snakebite-envenoming.
3. Pithayanukul P, Leanpolchareanchai J, Saparpakorn P. Molecular docking studies and anti-snake venom metalloproteinase activity of Thai mango seed kernel extract. *Molecules*. 2009; 14(9):3198-3213. doi: 10.3390/molecules14093198.

4. Leanpolchareanchai J, Pithayanukul P, Bavovada R, et al. Molecular docking studies and anti-enzymatic activities of Thai mango seed kernel extract against snake venoms. *Molecules*. 2009; 14(4):1404-1422. doi: 10.3390/molecules14041404.
5. Chinnasamy S, Chinnasamy S, Nagamani S, et al. Identification of potent inhibitors against snake venom metalloproteinase (SVMP) using molecular docking and molecular dynamics studies. *J. Biomol. Struct. Dyn.* 2015; 33(7):1516-1527. doi: 10.1080/07391102.2014.963146.
6. Srinivasa V, Sundaram MS, Anusha S, et al. Novel apigenin based small molecule that targets snake venom metalloproteases. *PLoS One.* 2014; 9(9):e106364. doi: 10.1371/journal.pone.0106364.
7. Hage-Melim LI, da Silva CH, Semighini EP, et al. Computer-aided drug design of novel PLA2 inhibitor candidates for treatment of snakebite. *J. Biomol. Struct Dyn.* 2009; 27(1):27-36. doi: 10.1080/07391102.2009.10507293.
8. World Health Organization. Guidelines for the Management of Snake-Bites [Online]. 2016. [cited 2020 Jan 28]. Available from: https://apps.who.int/iris/handle/10665/249547.
9. Félix-Silva J, Silva-Junior AA, Zucolotto SM, et al. Medicinal Plants for the Treatment of Local Tissue Damage Induced by Snake Venoms: An Overview from Traditional Use to Pharmacological Evidence. *Evid. Based Complement Alternat. Med.* 2017; 2017:5748256. doi: 10.1155/2017/5748256.
10. Omara T, Kagoya S, Openy A, et al. Antivenin plants used for treatment of snakebites in Uganda: ethnobotanical reports and pharmacological evidences. *Trop. Med. Health.* 2020; 48:6. doi: 10.1186/s41182-019-0187-0.
11. Elmaki NM, Al Sadawi IA, Hermann A, et al. Potential molecular docking of four acetylcholinesterase inhibitors. *Drug Designing & Intellectual Properties International Journal*. 2018: 191-194. doi: 10.32474/DDIPIJ.2018.02.000136.
12. Nadri MH, Salleh WM. Molecular Docking Studies of Phytochemicals from Piper Species as Potential Dual Inhibitor of Group X Secreted Phospholipase A2 (SPLA2-X) and Cyclooxygenase-2 (COX-2). *Res. J. Pharm. and Tech.* 2020; 13(5):2181-2186. doi: 10.5958/0974-360X.2020.00392.3.
13. Arafat A, Arun A, Ilamathi M, et al. Homology modeling, molecular dynamics and atomic level interaction study of snake venom 5′ nucleotidase. *J. Mol. Model.* 2014; 20(3):2156. doi: https://doi.org/10.1007/s00894-014-2156-1.
14. Eweas AF, Alhossary AA, Abdel-Moneim AS. Molecular docking reveals ivermectin and remdesivir as potential repurposed drugs against SARS-CoV-2. *Front. Microbiol.* 2021:3602. doi: https://doi.org/10.3389/fmicb.2020.592908.
15. Mohamed EM, Hetta MH, Rateb ME, et al. Bioassay-Guided Isolation, Metabolic Profiling, and Docking Studies of Hyaluronidase Inhibitors from Ravenala madagascariensis. *Molecules.* 2020; 25(7):1714. doi: 10.3390/molecules25071714.
16. Escalante T, Franceschi A, Rucavado A, et al. Effectiveness of batimastat, a synthetic inhibitor of matrix metalloproteinases, in neutralizing local tissue damage induced by BaP1,

a hemorrhagic metalloproteinase from the venom of the snake Bothrops asper. *Biochem. Pharmacol.* 2000; 60(2):269-274. doi: https://doi.org/10.1016/S0006-2952(00)00302-6.

17. Siddiqui S, Siddiqui BS, Naeed A, et al. Three pentacyclic triterpenoids from the leaves of *Plumeria obtusa. J. Nat. Products.* 1990; 53(5):1332-1336. doi: 10.1021/np50071a029
18. Aung HT, Aye MM, Thu ZM, et al. Bioactive Constituents from the Rhizomes of *Sansevieria cylindrica*. *Rec. Nat. Prod.* 2020; 14(4):269-275. doi: 10.25135/rnp.160.19.10.1440.
19. Dallakyan S, Olson AJ. Small-molecule library screening by docking with PyRx. Methods *Mol. Biol.* 2015; 1263:243-250. doi: 10.1007/978-1-4939-2269-7_19.
20. Trott O, Olson AJ. AutoDock Vina: improving the speed and accuracy of docking with a new scoring function, efficient optimization, and multithreading. *J. Comput. Chem.* 2010; 31(2):455-461. doi: 10.1002/jcc.21334.
21. Huang SY, Grinter SZ, Zou X. Scoring functions and their evaluation methods for protein-ligand docking: recent advances and future directions. *Phys. Chem. Chem. Phys.* 2010; 12(40):12899-12908. doi: 10.1039/c0cp00151a.
22. Santhosh MS, Hemshekhar M, Sunitha K, et al. Snake venom induced local toxicities: plant secondary metabolites as an auxiliary therapy. *Mini. Rev. Med. Chem.* 2013; 13(1):106-123.
23. Melo PA, Do Nascimento MC, Mors WB, et al. Inhibition of the myotoxic and hemorrhagic activities of crotalid venoms by Eclipta prostrata (Asteraceae) extracts and constituents. *Toxicon.* 1994; 32(5):595-603. doi: 10.1016/0041-0101(94)90207-0.